Thermodynamic Analysis of Chalk–Brine–Oil Interactions

Eftekhari, Ali Akbar; Thomsen, Kaj; Stenby, Erling Halfdan; Nick, Hamidreza M.

Published in:
Energy and Fuels

Link to article, DOI:
10.1021/acs.energyfuels.7b02019

Publication date:
2017

Document Version
Peer reviewed version

Thermodynamic analysis of chalk-brine-oil interactions[1]

Ali A. Eftekhari[*,1], *Kaj Thomsen*[2], *Erling H. Stenby*[3], *Hamidreza M. Nick*[4]

[1,4] Centre for Oil and Gas, Technical University of Denmark, Electrovej building 375, 2800 Kgs. Lyngby, Denmark; aliak@dtu.dk; hamid@dtu.dk

[2] Department of Chemical and Biochemical Engineering, Technical University of Denmark, Søltofts Plads, Building 229, room 204, 2800 Kgs. Lyngby, Denmark; kth@kt.dtu.dk

[3] Department of Chemistry, Technical University of Denmark, Kemitorvet 207, Building 206, room 240, 2800 Kgs. Lyngby, Denmark; ehst@kemi.dtu.dk

KEYWORDS

Low-salinity, zeta-potential, surface-complexation, reactive-transport.

ABSTRACT The surface complexation models (SCM) are used successfully for describing the thermodynamic equilibrium between the pure calcite surface (carbonate and calcium sites) and brine solutions. In this work, we show that the model parameters that are reported for the calcite-

[1] Please cite as "Eftekhari AA, Thomsen K, Stenby EH, Nick HM. Thermodynamic analysis of chalk-brine-oil interactions. Energy & Fuels. 2017 Oct 17, **DOI:** 10.1021/acs.energyfuels.7b02019"

http://pubs.acs.org/doi/abs/10.1021/acs.energyfuels.7b02019

brine system are not applicable to the natural carbonates. We adjust the SCM reaction equilibrium constants by fitting the model to the zeta potential data that are reported for the pulverized Stevns Klint chalk. Then, we use the model, implemented in PhreeqcRM geochemistry package coupled with a finite volume solver, to predict the breakthrough composition of different ions in the chromatographic experiments on the intact Stevns Klint chalk cores. Again, the model falls short in predicting the reactive transport of brine in a natural carbonate, implying that zeta potential data is not enough for optimizing the SCM model parameters for the reactive transport applications. We propose an optimization procedure that fits the coupled SCM-transport model parameters to the chromatographic (single-phase core flooding) data. The zeta potential measurements are implemented in the optimization scheme as nonlinear constraints. We then use the optimized model to study the thermodynamic equilibrium between the oil and chalk surfaces in presence of different brine compositions, including the dissolution and precipitation of minerals. We represent the chalk-oil interactions by acid-base equilibrium reactions between the calcium and carbonate sites on the chalk surface and carboxylic acids and amine bases on the oil surface, respectively. Comparing the model results to a data set of the spontaneous imbibition experiments for chalk shows that the remaining oil saturation in the imbibition experiments is correlated with the number of bonds between the amine and carboxylate groups on the oil surface and the carbonate and protonated calcium on the chalk surface.

Introduction

Reducing the remaining saturation of oil in a water-flooded core by injecting brine with modified electrolyte concentrations, is previously demonstrated in numerous experiments for various rock/oil/brine compositions in different temperatures and pressures (e.g., [1–4]). The mechanism by which oil is mobilized in presence of brine with a modified ionic composition is not yet understood

[2]. Migration of fine particles [5,6], rock dissolution [7], and surface charge modifications due to ion-exchange and surface complexation reactions [8–10] are among the possible mechanisms. Each one of these mechanisms, although still under investigation, is relatively well known. Various mathematical and thermodynamic models exist that can adequately (e.g., fine migration) and often accurately (e.g., dissolution/precipitation) describe the underlying physics of each process. The major gap, however, is a link between the physical aspects of these mechanisms and the transport properties (i.e., relative permeability) of the aqueous and oleic phase in porous media. Until now, this gap is filled by using empirical relations, often with one or few unknown parameters that are later estimated by fitting the model to the core flooding experimental data (also known as history matching [11–14]).

The other major issue in the mechanistic models, particularly in the interactions of rock-oil-brine which are described by ion exchange or surface complexation models, is the uncertainty of the physical parameters. For instance, the adsorption of ions on the surface of calcite can be described accurately by surface complexation models [15,16]. These models come in different flavors [17], each with its own sets of assumptions and limitations. Moreover, each model requires several equilibrium constants that are often only measured for a very specific system. Since these models are the foundation of the mechanistic models of the modified salinity water flooding, the choice of model and its physical parameters can dramatically affect the transport properties of oil and water in porous media and the predictive capabilities of the model.

In this work, we attempt to address both problems; first we suggest a procedure for optimizing the SCM parameters by fitting the model to the chromatographic experiments and zeta-potential measurements, considering the dissolution of the chalk (calcite) surface and the possible precipitation of anhydrite in presence of sulfate ion. We also investigate the influence of silica and

clay particles, that is observed on the surface of the North Sea chalk[18–20], on the surface charge of the chalk particles and the adsorption of ions in the chromatographic tests. Secondly, we apply the model to a set of spontaneous imbibition tests to predict the thermodynamic equilibrium between the oil and chalk surfaces in presence of different brine composition, to find a correlation between the surface properties of oil and carbonate (predicted by the model) and the remaining oil saturation (measured experimentally).

Mathematical model

The mathematical models are presented here in two subsections. First, we describe the thermodynamic equilibrium model for the chalk-brine-oil system. Then, we present the model for the multi-component reactive transport of brine in a carbonate porous medium.

Chalk-oil-brine interactions

It is generally accepted that oil and rock surfaces interact through a water-film. The ions in the water film get adsorbed on the functional group such as hydroxylated calcium or carbonate on the chalk surface [15] and the carboxylic acids or amine bases on the surface of oil [21]. These functional groups can also undergo the dissociation and protonation reactions that change the surface charge. Moreover, the adsorption/desorption of ions to/from the surface can change the three dimensional structure of the surface, i.e., precipitation/dissolution [17]. It is previously shown that a surface complexation model, which "gives a molecular description of the adsorption of ions using a thermodynamic equilibrium approach" [17], provides promising results in fitting the experimental results of the adsorption of ionic species on the pure crystalline chalk samples. A detailed review and formulation of the surface complexation models can be found elsewhere [17]. In this work, we

use a diffuse-layer model, with the equilibrium reactions that are shown in Table 1. The stability constants for these reactions for the system of brine and calcite are measured [15,16,22] or estimated [7,8] by various investigators and repeated here in Table 2for convenience. For the oil-brine system, there are no reported measurements in the literature to the best of our knowledge. Therefore, we follow other investigators [8,23] and use the equilibrium constants of the analog aqueous phase reactions of the carboxylate and amine groups.

Table 1. Surface complexation reaction between the ionic species in brine and the oil and chalk surface sites

Surface site	**#**	**Surface complexation**
Carbonate:	1	$>CO_3H \leftrightarrow >CO_3^- + H^+$
$>CO_3H$	2	$>CO_3H + Ca^{2+} \leftrightarrow >CO_3Ca^+ + H^+$
	3	$>CO_3H + Mg^{2+} \leftrightarrow >CO_3Mg^+ + H^+$
Calcite:	4	$>CaOH + H^+ \leftrightarrow >CaOH_2^+$
>CaOH	5	$>CaOH \leftrightarrow CaO^- + H^+$
	6	$>CaOH_2^+ + CO_3^{2-} \leftrightarrow >CaCO_3^- + H_2O$
	7	$>CaOH_2^+ + SO_4^{2-} \leftrightarrow >CaSO_4^- + H_2O$
	8	$>CaOH_2^+ + HCO_3^- \leftrightarrow >CaHCO_3 + H_2O$
-NH	9	$-NH + H^+ \leftrightarrow -NH_2^+$
-COOH	10	$-COOH + H^+ \leftrightarrow -COO^- + H^+$
	11	$-COOH + Na^+ \leftrightarrow -COONa + H^+$
	12	$-COOH + K^+ \leftrightarrow -COOK + H^+$
	13	$-COOH + Ca^{2+} \leftrightarrow -COOCa^+ + H^+$
	14	$-COOH + Mg^{2+} \leftrightarrow -COOMg^+ + H^+$
	15	$-COOH + Ba^{2+} \leftrightarrow -COOBa^+ + H^+$

Table 2 shows the stability constants and the standard enthalpy of reaction for the surface complexation reactions between the surface sites of chalk and the ionic species in brine. For the oil phase, we use the LLNL database of PHREEQC for the reactions between the metal ions and the acetate ion.

Table 2. Equilibrium constants for the chalk-brine surface complexation reactions; please note that some of the constants are not reported in the cited publications, e.g., for sulfate reaction. These values are either estimated from the analog reactions or replaced by values reported in other references. The enthalpy of reactions are estimated using the Van't Hoff equation for the equilibrium reactions reported by Hiorth et al. [7] at different temperatures. Please see the original manuscripts for more details. The reactions stoichiometry are shown in **Table 1**

References	[7]	[8]	[24]	[16]	[25]	[7]	[8]	[25]
Reaction #			logK			$\Delta H \left[\frac{kJ}{mol}\right]$		
1	-4.9	-5.1	-5.1	-4.9	-0.67	8.706	8.86	-37.91
2	-3.16	-2.6	-1.7	-2.8	-3.16	15.67	21.708	15.67
3	-3.17	-2.2	-2.2	-2.2	-3.17	17.41	13.833	17.41
4	12.9	11.8	11.5	12.2	12.9	-82.71	-68.83	-82.71
5	-17	-17	-12	-17	-17	0.0	0.0	0.0
6	3.32	4.9	5.6	4.9	3.32	14.91	10.717	14.91
7	2.1	2.1	2.89	2.89	1.64	14.44	18.725	-1.49
8	0.96	0.96	1.66	1.61	0.96	13.51	14.933	13.51

Single-phase multi-component reactive flow in carbonate

The multi-component reactive flow of brine in a carbonate porous medium can be written as

$$\frac{\partial}{\partial t}\left(\varphi c_i + (1-\varphi)\rho_s a_s q_i\right) + \nabla.\left(\mathbf{u}_w c_i\right) + \nabla.\left(-\varphi D_i \nabla c_i\right) = R_i, \qquad (1)$$

where φ [-] is the porosity, c_i [mol/m^3] is the molar concentration of species *i* in the aqueous phase, ρ_s [kg/m^3] is the density of the rock, a_s [m^2/kg] is the specific surface area of the porous medium, q_i [mol/m^2] is the concentration of the adsorbed species *i*, $\mathbf{u}_\alpha$ [m/s] is the velocity vector of the water phase, D_i [m^2/s] is the diffusion coefficient of species *i* in the aqueous phase, and R_i [mol/(m^3.s)] is a source/sink term. The relation between the concentration in the aqueous phase and the concentration on the surface comes from the SCM that is described in the previous section.

Dissolution and precipitation

The dissolution and precipitation of calcite ($CaCO_3$) and anhydrite ($CaSO_4$) are suggested to change the recovery of oil from chalk cores. Anhydrite is not directly found in chalk, but can form due to the reaction between the sulfate-rich injected brine and the calcium-rich insitu brine. Various mechanisms including the formation and migration of fine particles are suggested to explain these experimental observations. Precipitation of anhydrite generates fine particles that may increase the production of oil [3,5,6] or damage the porous medium [26]. Mathematical modelling of the fine migration phenomenon is outside the scope of this paper. However, from a thermodynamic point of view, we compare the accuracy of various thermodynamic models, i.e., Debye-Hückel, [27], and Pitzer [28] with the more sophisticated Extended UNIQUAC model [29–31] in predicting the solubility of anhydrite and calcite in brine at reservoir conditions.

The dissolution/precipitation of calcite decreases/increases the number of surface sites, which affects the adsorption and desorption of ions to/from the chalk surface. Moreover, the dissolution

of anhydrite can affect the recovery of oil by increasing the sulfate content in the aqueous phase which consequently alters the wettability of chalk. Hence, we include the dissolution/precipitation of calcite and anhydrite in our transport model.

Oil-chalk interactions

According to Buckley et al. [32], when a water film is present between oil and rock and in the absence of heavy polar components in the oil phase, e.g., asphaltenes that can precipitate on the rock surface, the only mechanisms for the adsorption of oil on the chalk surface is the acid-base interaction of the charged complexes that are formed on the surface of oil and chalk. These interactions can also occur between the surface complexes that are masked by the potential determining ions. In this work, we only consider the acid-base interactions, which can be described by the following reactions:

$$>CaOH_2^+ + \ -COO^- \leftrightarrow \ >CaOH_2-COO-,\ \log k_{eq} = -1.51,\ \Delta H = 4.96 \text{ kJ/mol} \qquad (2)$$

$$>CO_3^- + -NH_2^+ \leftrightarrow \ >CO_3-NH_2-,\ \log k_{eq} = 1.76,\ \Delta H = -25 \text{ kJ/mol} \qquad (3)$$

The equilibrium constants for the above reactions are estimated from the analogous aqueous phase reactions. The interactions between the complexes that are masked by the potential determining ions will be covered in a future work. The activity of each surface species in the above reactions are assumed to be equal to their mole fraction, i.e., the fraction of a surface type that is occupied by one of the reactants in reactions (2) and (3). The standard state is defined as a mole fraction of one, i.e., when a surface species fully occupies a given surface site [33].

Optimizing stability constants for the surface complexation reactions

The stability constants that are reported for the chalk-brine surface complexation reactions are measured for the pure crystalline calcite samples. However, a chalk reservoir sample is not

composed of pure calcite, and the stability constants need to be adjusted for the model to more accurately represent the brine-chalk interactions. To that end, we optimize the stability constants of the surface complexation reactions (see Table 1) to fit the predicted surface charge to the measured zeta potential of the Stevns Klint chalk reported by [4,34,35]. Zhang and co-workers used the Stevns Klint chalk samples that was milled in a ball mill for 48 hours to make a 4.0wt% suspension of chalk in a 0.573 mol/l NaCl solution. They adjust the concentration of the potential determining ions by adding concentrated solutions of $CaCl_2$, $MgCl_2$, or Na_2SO_4, and keep the pH constant at 8.4 by adding few drops of HCl or NaOH. They measure the zeta potential at different PDI concentrations using an AcoustoSizer from Matec applied science. Zhang et al. did not report whether their experimental set-up is open to the atmosphere; however, the negative value of the zeta potential measured in the absence of sulfate at pH 8.4 indicates the presence of carbonate and bicarbonate ions in the solution, which is the result of the dissolution of the atmospheric CO_2 in the suspension [36]. Therefore, we assume that the suspension is in equilibrium with the atmospheric CO_2 with a partial pressure of 39 Pa. The zeta potential cannot be directly calculated from a surface complexation model. However, Megawati et al. [25] suggested the following relation for estimating the zeta potential, i.e., the potential at the shear plane (ζ [V]) is calculated by assuming that the shear plane is located at a known distance from the stern layer surface potential:

$$\zeta = \psi\left(\kappa_\zeta\right) = \psi_0 \exp\left(-\kappa_\zeta / \kappa^{-1}\right), \qquad (4)$$

where κ^{-1} [m] is the Debye length, and κ_ζ [m] is assumed to be 3×10^{-10} m. We found that using the above assumption only slightly changes the results.

For fitting the SCM model to the zeta potential measurements, we minimize the following objective function (OF_ζ) by changing the model parameters no more than ±20% of their original value:

$$OF_\zeta = \sum_{i=1}^{N_\zeta} \left(\zeta_i^{\text{exp}} - \zeta_i^{\text{calc}} \right)^2, \qquad (5)$$

subject to the following set of nonlinear constraints:

$$\zeta_i^{\text{calc}} \zeta_i^{\text{exp}} \geq 0 \quad \text{for } i = 1, \ldots, N_\zeta. \quad (6)$$

In the above equation, N_ζ denotes the number of data points (here 76) and the superscripts 'exp' and 'calc' denote the experimental and calculated values of the zeta potential, respectively. It is important that the model does not predict a positively charged surface for a chalk surface that is negatively charged, and vice versa, since the surface charge is shown to be directly related to the recovery of oil in the carbonates [34–36]. Therefore, we define the nonlinear inequality constraints shown by Eq. (6). The objective function is written in Julia language [40], which utilizes the PHREEQC reaction module PhreeqcRM [41] with the help of a Julia wrapper JPhreeqc.jl [42]. For the minimization, we use the SLSQP algorithm [43,44] for nonlinearly constrained gradient-based optimization from the NLopt package [45].

Effect of clay on the surface potential

The presence of nanometer scale clay crystals that is observed on the surface of chalk can have a considerable effect on the average charge of the chalk surface. We include different amount of clay in our surface complexation model. The surface complexation reactions of the Kaolinite edges, reported by Brady and Krumhansl[46] is used to represent the clay particles. We assume that the clay nanocrystals are homogeneously distributed on the chalk particles. We then calculate the

average surface charge by

$$\sigma = \frac{\left(1-w_{clay}\right)a_{calcite}\sigma_{calcite} + w_{clay}a_{clay}\sigma_{clay}}{\left(1-w_{clay}\right)a_{calcite} + w_{clay}a_{clay}}, \tag{7}$$

where w_{clay} [-] is the mass fraction of clay in chalk sample, a_{clay} [m^2/g] is the specific surface area of clay, σ [C/m^2] is the average surface charge of chalk, and $\sigma_{calcite}$ [C/m^2] and σ_{clay} [C/m^2] are the surface charge of calcite and clay surfaces, respectively. The surface potential (ψ_0 [V]) of the chalk particles can be calculated by

$$\psi_0 = \frac{2RT}{F}\operatorname{arcsinh}\left(\sigma\left(8\varepsilon_0\varepsilon RTI\right)^{-\frac{1}{2}}\right), \tag{8}$$

where F [96485.33289 C/mol] is the Faraday constant, R [8.314 J/(mol.K)] is the gas constant, T [K] denotes temperature, ε_0 [$8.854187817\times10^{-12}$ C/(V.m)] is the vacuum permittivity, ε [-] is the dielectric constant of the solution, and I [mol/m^3] denotes the ionic strength.

Results and discussion

In this section, we first present the result of the optimization of the surface complexation model parameters. Then we use the optimized parameters to model the single phase reactive flow of brine in chalk (e.g., chromatographic experiments [47]) and demonstrate how sensitive the breakthrough curves of different ions are to the model parameters. Then we tune the model parameters to the chromatographic experimental data of flow of brine in chalk and use the tuned model parameters to find a relation between the recovery of oil when changing the salinity of the injected brine and the number of bonds between the carboxylate group on the oil surface and the protonated calcium sites on the chalk surface.

Optimized parameters of the surface complexation model

We use the experimental data of Zhang et al.[35], who measured the zeta potential of a 4 wt% mixture of pulverized Stevns Klint chalk particles in brine with different ionic compositions. They do not report whether the system is open to the atmosphere during the measurements. Therefore, we assume that the system is in contact with the atmospheric CO_2. The carbonate and calcium site densities ($c_{calcium}$ and $c_{carbonate}$), i.e., number of surface sites per unit area of the chalk surface, are not reported. Therefore, we use the surface densities of 2.0 to 5.0 #/nm^2 [7]. The specific surface area of chalk (natural calcite) is reported as 2.0 m^2/g [1,18]. However, we study the effect of the specific surface area on the optimization results, by varying it from 2.0 to 5.0 m^2/g. We run the optimization routine for each pair of specific surface area and surface site density of chalk.

The results of fitting the diffuse-layer surface complexation model to the zeta potential data are reported in Table 3. Note that the concentration of sulfate and carbonate ions are kept almost constant in the zeta potential measurements of Zhang et al.[35]. Therefore, the equilibrium constants for the reactions 7 and 8 are not modified by the optimization algorithm. As it was previously observed by Hiorth et al.[7], a better fit (lower sum of square of errors) is obtained by using a surface site density of 2.0 #/nm^2. Increasing the total surface area slightly reduces the error, but it does not result in a significant better fit. Overall, the fit has a normalized error of 4.75 mV which is not excellent but acceptable. The nonlinear constraint of Eq. (6) enables the calibrated model to predict the sign of the zeta potential (and surface charge) correctly. None of the equilibrium constants that are reported in the literature (see Table 2) can predict the correct sign of the surface charge for the whole range of experimental data that is used in this study.

Table 3. Optimized parameters for the equilibrium constants of calcium and carbonate surface complexation reactions; the stoichiometry of reactions 1-8 are shown in **Table 1**; optimization errors are calculated using a t-test with numerically-estimated Jacobian matrix.

$a_{calcite}$ (m^2/g)		**2**	**2**	**3**	**3**	**4**	**4**	**5**	**5**
$c_{calcium}$, (#/nm^2)	$c_{carbonate}$	2	5	2	5	2	5	2	5
	Reaction								
Equilibrium constant	1	-4.00±0.0000	-4.05	-4.00	-4.03	-4.11	-4.05	-2.76	-4.02
	2	-2.47±0.0000	-2.55	-2.55	-2.55	-2.55	-2.55	-1.20	-2.55
	3	-2.38±0.0008	-2.61	-2.60	-2.62	-2.46	-2.60	-1.10	-2.62
	4	14.08±0.0000	16.71	14.17	14.02	14.45	16.79	14.47	18.01
	5	-17.09±0.0002	-16.95	-17.36	-17.53	-16.81	-23.46	-17.14	-17.43
	6	3.33±0.0000	3.28	3.15	3.23	3.40	3.29	3.39	3.20
	7	1.45±0.0001	1.45	1.45	1.45	1.45	1.45	1.45	1.45
	8	0.48±0.0000	0.48	0.48	0.48	0.48	0.48	0.48	0.48
error (mV)		4.78	5.82	4.88	5.83	4.75	5.81	4.75	5.82

The optimum values of zeta potential are plotted against the experimental data in Figure 1, with and without the nonlinear constraint of Eq. (6). The solid blue line depicts the zero error, i.e., calculated zeta potential is equal to the measured values. The unconstrained optimization (Figure 1-b) gives a better fit of the model to the experimental data. However, near the point of zero-charge (i.e., zeta potential of zero) the model predicts the sign of the surface charge incorrectly. On the other hand, the model parameters obtained from the constrained optimization produces larger error in the prediction of the zeta potential on the chalk surface. This error may fall within the range of the uncertainty of the measured zeta potentials; since the measurement errors are not reported by Zhang et al. [35], we cannot confirm this, even though large errors are observed during the measurement of the zeta potential specially for a suspension that is close to coagulation condition, i.e., with an absolute value of zeta potentials below 30 mV [48]. A larger discrepancy can also be observed between the model prediction and the experimental data for the negative values of zeta

potential. This can be attributed to the dissolution of the atmospheric CO_2 in the solution during the zeta potential measurements. Moreover, other SCM's with different complexation reaction can be considered, e.g., Song et al.[49] to find the best model that represents the chalk-brine interactions.

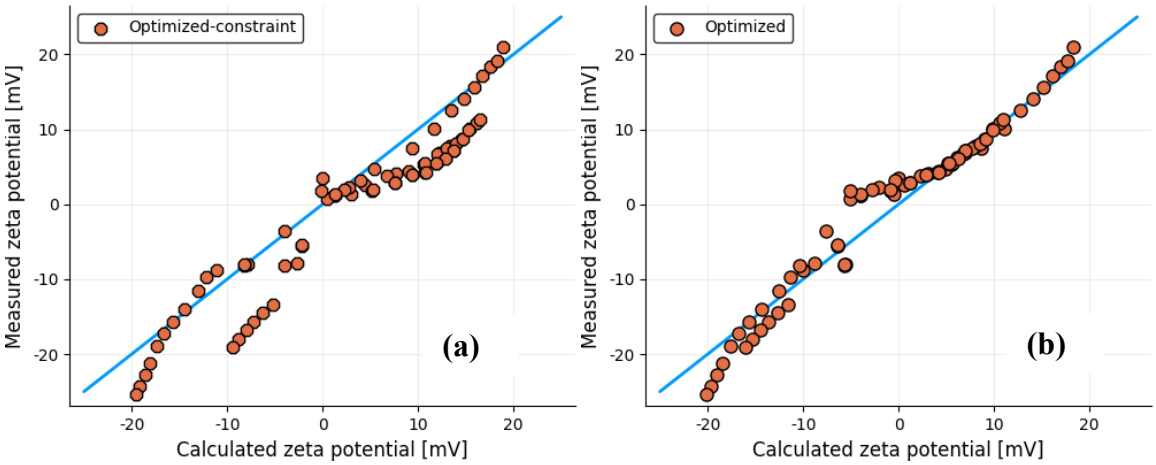

Figure 1. Measured values of zeta potential plotted against the calculated values using a diffuse layer surface complexation model with the reaction equilibrium constants that are optimized: (a) with and (b) without the nonlinear constraints of Eq. (6).

Effect of clay on the zeta potential calculations

The effect of the presence of 0.2 wt% and 1.0 wt% of clay particles (in the form of Kaolinite edges) are shown in Figure 2. The clay nanoparticles on the surface of chalk are negatively charged at pH 8.4, which decreases the calculated average zeta potential of the chalk surface. According to our SCM model, in the absence of clay particles, the negative surface charge for chalk surface can only be attained in presence of carbonate and sulfate ions (or in impractically high pH). However, if a substantial amount of clay is present on the chalk surface, the chalk surface can be negatively charged even in the absence of carbonate and sulfate ions in the brine. Although the amount of clay on the Stevns Klint outcrop samples is not determined by Zhang et al.[4], the fact that they

observed negative values of zeta potential only in presence of sulfate and carbonate ions indicates that the amount of clay on the chalk surface is probably negligible.

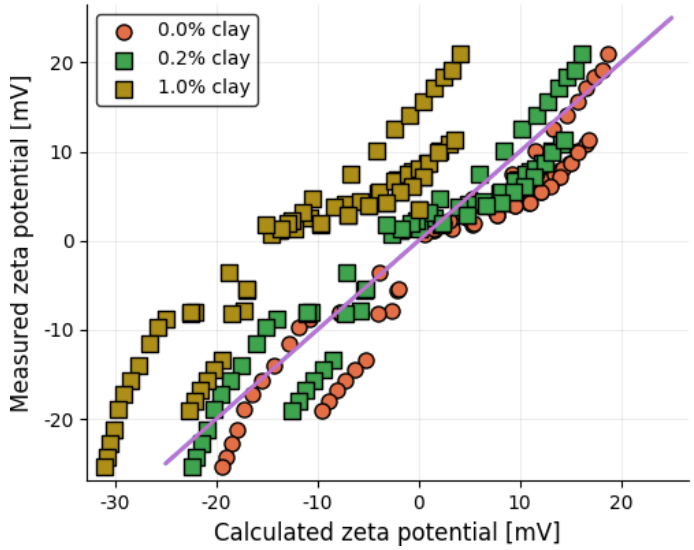

Figure 2. Effect of clay particles on the calculated zeta potential of the chalk surface; the green and brown square markers show the calculated zeta potential in presence of 0.2 wt% (see Hjuler and Fabricius[18]) and 1.0 wt% Kaolinite edge, respectively, versus the measured zeta potential on the Stevns Klint chalk surface.

Effect of thermodynamic models on the prediction of solubility

The experimental solubility of anhydrite in water at different temperatures and a maximum pressure of 8 bar are shown in Figure 3. The experimental data is compared with the predictions of three thermodynamic model, i.e., Davies [33] and Pitzer [50], both from PHREEQC and the well-established Extended UNIQUAC from the ScaleCERE software [30,31]. The results show that at lower temperatures, both Davies and Pitzer models overestimate the solubility of anhydrite by around 20%. However, both models give a reasonable approximation of the solubility at higher temperatures (which are close to the reservoir conditions). This observation becomes important when we consider the high computation cost of the more complicated Pitzer and Extended

UNIQUAC, compared to the simple Davies model. In the computationally expensive simulation of the reactive flow in porous media, one can use the simple Davies (or alternatives) without compromising the accuracy.

The effect of higher pressures on the activity of the ionic species in the liquid phase and the solubility is discussed elsewhere [50–52]. Here we emphasize that the Davies model does not consider the effect of pressure on the solubility and must be used with caution at higher pressures.

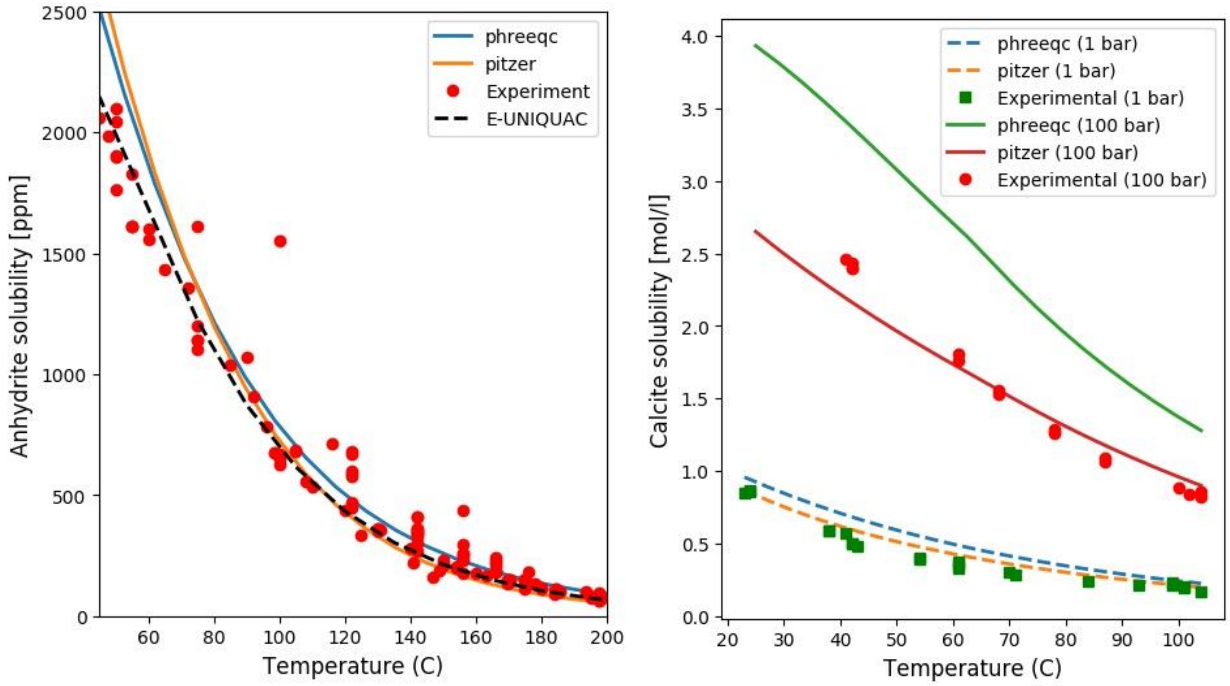

Figure 3. Experimental data for the solubility of anhydrite (left) and calcite (right) in water at different temperatures; for anhydrite the pressure is 8 bar (red circles); for calcite, the system is in equilibrium with CO_2 at 1 bar (green squares) and 100 bar (red circles); the lines show the prediction of solubility by the Davies, Pitzer, and Extended UNIQUAC models, as indicated in each figure.

Modeling the single-phase flow of brine in chalk

We use finite volume method to discretize the advection-diffusion Eq. (1) to a system of algebraic equations. The diffuse-layer surface complexation model in PhreeqcRM describes the relation between the concentration in the aqueous phase (c_i) and on the chalk surface (q_i). Similar to Nick et al. [53], the operator splitting technique is implemented, which first solves the advection equation, then the diffusion equation and finally the reaction equations (surface complexation model). The initial and boundary conditions are similar to those described in the experimental work of [34]. In their experiments, they first saturate a Stevns Klint chalk core (0.037 m diameter, 0.070 m length, porosity of 0.49, and permeability of 0.002×10^{-12} m^2) with a 0.573 mol/l NaCl solution (with no Ca and Mg ions). Then, with a rate of 0.2 ml/min, they inject a brine solution that contains Ca, Mg, and SCN^- tracer and measure the concentration of the ions at the outlet in different times.The concentration of the initial and the injected brine is shown in Table 5.

Table 4. Values of the equilibrium constants optimized to fit the zeta potential measurements and the adjusted values to match the concentration history in a chromatographic experiment

Reaction #	1	2	3
Equilibrium constant (zeta potential)	-4.00	-2.47	-2.38
Equilibrium constant (concentration history)	-4.50	-1.29	-2.04

Table 5. The initial and injected brine compositions in the chromatographic experiments of Zhang et al. [34]

Concentration (mol/l)	Na^+	K^+	Mg^{+2}	Ca^{+2}	Cl^-	HCO_3^-	SO_4^{-2}	SCN^-	pH

Injected	0.504	0.0	0.013	0.556	0.0	0.0	0.0	0.013	8.4
Initial	0.573	0.0	0.0	0.0	0.573	0.0	0.0	0.0	8.4

In our simulations, the diffusion coefficient is assumed to be the same for all the species. It is obtained by fitting the model to the tracer concentration history. **Figure 4**-a shows the concentration history of Ca^{2+}, Mg^{2+}, and SCN^{-}. One can observe that the surface complexation model, with parameters that are tuned to the zeta potential data, is not able to correctly capture the adsorption and desorption of calcium and magnesium on the chalk surface. By adjusting the equilibrium constants for the reactions 1 to 3, the model matches the measured concentration history of the ions, as shown in **Figure 4**-b. The adjusted equilibrium constants are shown in Table 4. The difference between the old and the new values shows that the equilibrium constants for reactions 1 and 3 are only slightly adjusted. However, the new equilibrium constant for reaction 2 is lower than its old value by a factor of 50%. One explanation is that the zeta potential is measured for a pulverized chalk, which can potentially change the surface properties of the original outcrop core. Therefore, the parameters that are obtained by fitting the surface complexation model to the pulverized chalk samples are not necessarily representative of the brine-chalk interactions in an intact core.

Additionally, we study the effect of the chalk specific surface area and the surface site densities. As expected, by increasing the value of these parameters the breakthrough of the Ca and Mg ions is delayed, i.e., the predicted breakthrough curves shift to the right. The results are shown in Figure 5 as the outlet concentration of each ion, C [mol/m^3], divided by the inlet concentration C_0 [mol/m^3] versus the number of injected pore volumes (PV) of brine.

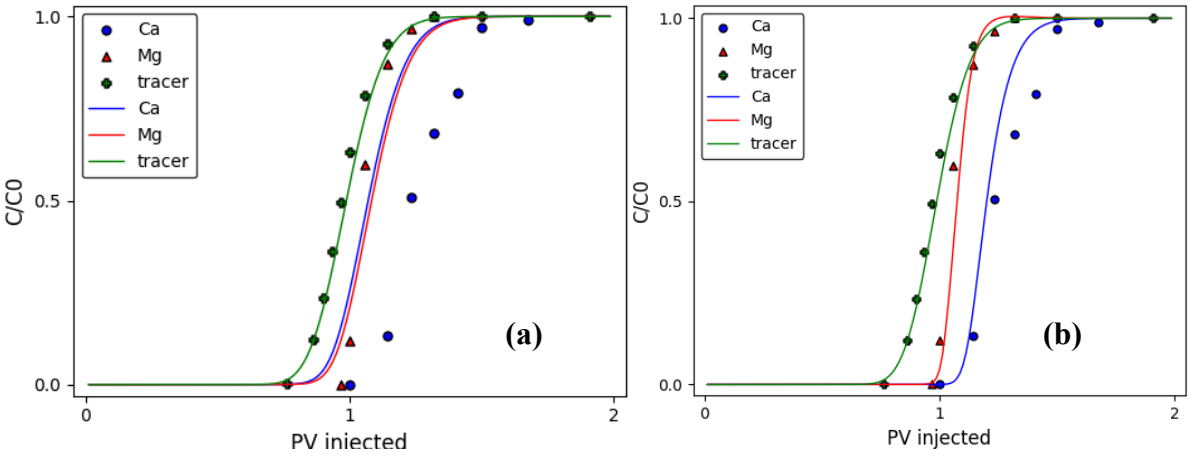

Figure 4. The measured (shown by markers) and calculated (shown by solid lines) normalized concentration history of Ca^{2+}, Mg^{2+}, and SCN^- (tracer) ions at the outlet of a Stevns Klint chalk core versus the number of injected pore volumes of brine: (a) the equilibrium constants fitted to the zeta potential data; (b) the equilibrium constants for reactions 1 to 3 are slightly adjusted to obtain a better match. The data is extracted from Figure 2 of Zhang et al. [34]

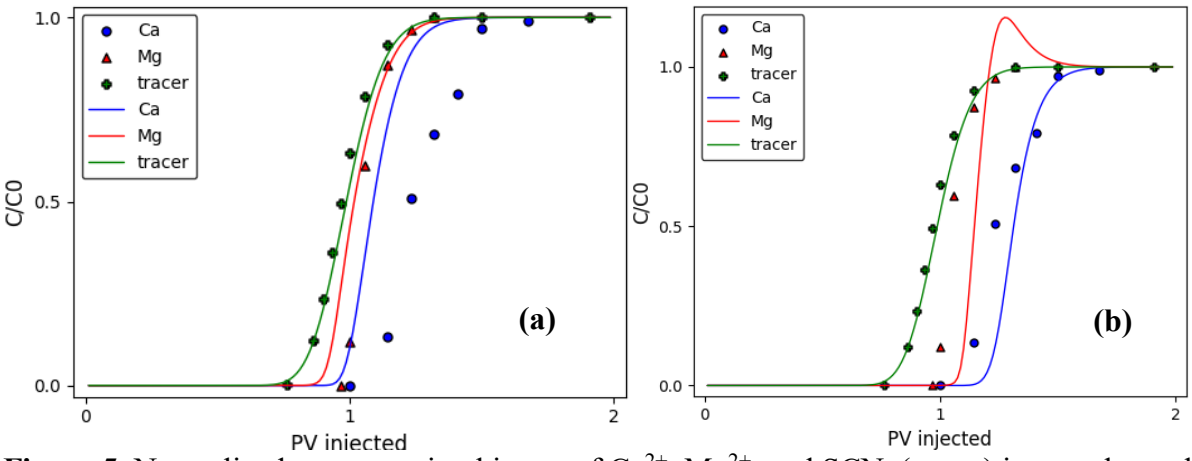

Figure 5. Normalized concentration history of Ca^{2+}, Mg^{2+}, and SCN^- (tracer) ions at the outlet of a Stevns Klint chalk core for a specific surface area of: (a) 1 m^2/g and (b) 3 m^2/g. The experimental data is from Zhang et al.[34]

Effct of clay on the adsorption of ions on the chalk surface

Figure 6 shows the effect of the presence of different amounts of Kaolinite edges in chalk on the adsorption of calcium and magnesium in the chromatographic tests of Zhang et al.[34]. By increasing the amount of clay from 0.1 wt% to 2.0 wt% and 5.0 wt%, the breakthrough of both Mg and Ca ions are further delayed, which is an indication of a higher adsorption of the metallic ions on the clay particles. However, considering the large surface area of the clay particles, i.e., 15 m^2/g, the presence of clay particles does not considerably affect the metal uptake compared to other physical parameters of the system, e.g., the specific surface area of calcite. Comparing these results with the dramatic effect of clay particles on the chalk surface potential, it can be concluded that at the temperature and pH range of these experiments, the interaction of the potential determining ions with the chalk surface is not affected by the presence of clay particles; however, small amount of clay particles that are evenly distributed on the chalk surface, dramatically decrease the zeta potential and surface charge of the chalk particles due to the larger equilibrium constant of the deprotonation reaction of the clay particles.

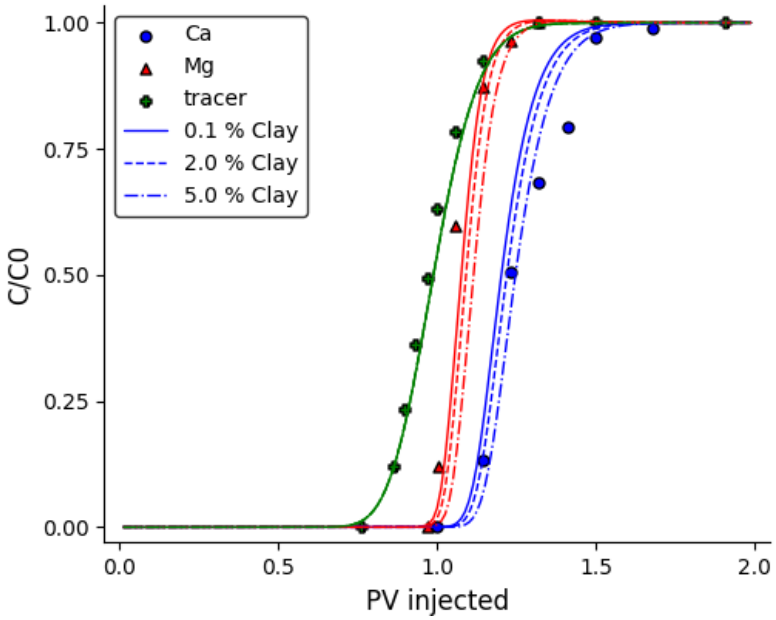

Figure 6. Effect of clay particles on the adsorption of Ca and Mg ions on the surface of chalk. The solid, dashed, and dashed-dotted lines show the adsorption history on a chalk core that contains 0.1 wt%, 2.0 wt%, and 5.0 wt% clay, respectively.

Oil recovery from the modified salinity brine-flooding in chalk

In the previous section, we show that the adsorption and desorption of ions on the surface of chalk can be described by a surface complexation model, although the model parameters need to be tuned to the single-phase flow experimental data. In this section, we use the optimized model parameters for the single phase flow experiments to study the imbibition experiments of Fathi et al. [1] and Zhang et al[34]. They cut 7 cm long core plugs with a diameter of 3.81 cm from an Stevns Klint outcrop block (porosity of 45%, permeability of 1-2 mD, and specific surface area of 2 m^2/g), cleaned the core with 250 ml of distilled water at 50 ^oC, and aged it with crude oil with the procedure described by Puntervold et al.[54]. The composition of the formation water is similar to the Valhall field, with a total dissolved solid of 62.80 g/l. The imbibing brine is made by modifying the ionic composition of the artificial seawater, as shown in Table 6. The crude oil is a mixture of

an acidic reservoir stabilized crude oil and 40 vol % heptane, centrifuged and filtered to separate its asphaltene content, with a total acid number of 1.90 mg KOH per gram oil[1]. The base number of the oil in the experiments of Fathi et al.[1] is zero. Zhang et al.[34], however, used two different types of oil which contains both acidic and basic components. The number of carboxylic acid and amine sites on the oil surface can be estimated by

$$c_{COOH} = 0.602 \times 10^6 \frac{AN}{1000 a_{oil} MW_{KOH}},$$

$$c_{NH} = 0.602 \times 10^6 \frac{BN}{1000 a_{oil} MW_{KOH}},$$

where 0.602×10^6 is the conversion factor from [mol/m^2] to [#/nm^2], c_{COOH} [#/nm^2] and c_{NH} [#/nm^2] denote the carboxylic acid and amine site densities, AN [mg KOH/g oil] and BN [mg KOH/g oil] denote the acid and base number of oil, respectively, MW_{KOH} [56.1 g/mol] is the molecular weight of potassium hydroxide, and a_{oil} [m^2/g] denotes the specific surface area of oil. The core initially is saturated with 10% formation water and 90% crude oil. Then the core is immersed in the imbibing fluid at different temperatures, i.e., 100, 110, and 120^{o}C at a pressure of 10 bar. Instead of modeling the whole imbibition process, we confine our interest to the ultimate recovery in the imbibition test, i.e., when the imbibed water in the core reaches a saturation at which the capillary pressure is zero and no more oil can be recovered. We solve the surface complexation model for the system of chalk, imbibing brine, and the initial oil in the core, to find the amount of $>CaOH_2^+$ and $>CO_3^-$ on the surface of chalk and $-COO^-$ and $-NH_2^+$ on the surface of oil. These values serve as the initial condition for the reactive system described by Eqs. (2) and (3). Since the equilibrium constants for these reactions are not reported in the literature, we use the equilibrium constant of the analog aqueous phase for these reactions. The composition of the

species $>CaOH_2-COO-$ and $>CO_3-NH_2-$ is an indication of the tendency of the oil phase to adsorb on and consequently remain in the chalk.

Table 6. Composition of the formation and the imbibing brine in the imbibition tests of Fathi et al. [1]

Ions (mol/l)	FW	SW	SW0NaCl	SW4NaCl	dSW1600	dSW10000	dSW20000	SW0T	SW1/2T	SW1T
HCO_3^-	0.009	0.002	0.002	0.002	0.000	0.001	0.001	0.002	0.002	0.002
Cl^-	1.07	0.525	0.126	1.726	0.027	0.158	0.314	0.583	0.538	0.492
SO_4^{2-}	0.00	0.024	0.024	0.024	0.001	0.007	0.014	0.000	0.012	0.024
SCN-	0.00	0.000	0.000	0.000	0.000	0.000	0.000	0.000	0.012	0.024
Mg2+	0.008	0.045	0.045	0.045	0.002	0.013	0.027	0.045	0.045	0.045
Ca2+	0.029	0.013	0.013	0.013	0.001	0.004	0.008	0.013	0.013	0.013
Na+	1.00	0.450	0.050	1.650	0.023	0.135	0.269	0.460	0.427	0.393
K+	0.005	0.010	0.010	0.010	0.001	0.003	0.006	0.010	0.022	0.034
Li+	0.000	0.000	0.000	0.000	0.000	0.000	0.000	0.000	0.012	0.024
Ionic strength	1.112	0.657	0.257	1.857	0.033	0.197	0.393	0.644	0.647	0.649
TDS (g/l)	62.80	33.39	10.01	103.53	1.67	10.02	20.00	33.39	33.39	33.39

Figure 7 shows the remaining oil saturation after imbibition test plotted against $>CaOH_2-COO-$ concentration, i.e., the number of bonds between the protonated calcium and the carboxylate group per unit contact area. The remaining oil saturation on the y-axis is obtained from the imbibition experiments of [1] and the concentration of the carboxylate ion adsorbed on the protonated calcium is calculated by means of our surface complexation model that is tuned to the single phase core flooding data (seeTable 4). The base number of the oil that is used in the imbibition experiments is zero; hence, the adsorption of amine groups on the carbonate sites does

not need to be considered. The equilibrium constant for the reaction described by Eq. (2) is obtained from the Gibbs energy of the analog aqueous phase reaction and is *not* adjusted to obtain the correlation depicted in Figure 7. This correlation shows that by decreasing the number of strong bonds between the oil and the chalk surfaces, the remaining oil in the imbibition experiments is decreased, i.e., the recovery of oil increases. In these particular experiments, this is done by lowering the salinity and increasing the sulfate concentration in the imbibing brine. The sulfate ion is adsorbed on the surface of chalk, which decreases the number of available protonated calcium sites that can react with the carboxylate ions and bind the oil phase to the chalk surface, as shown in Figure 8.

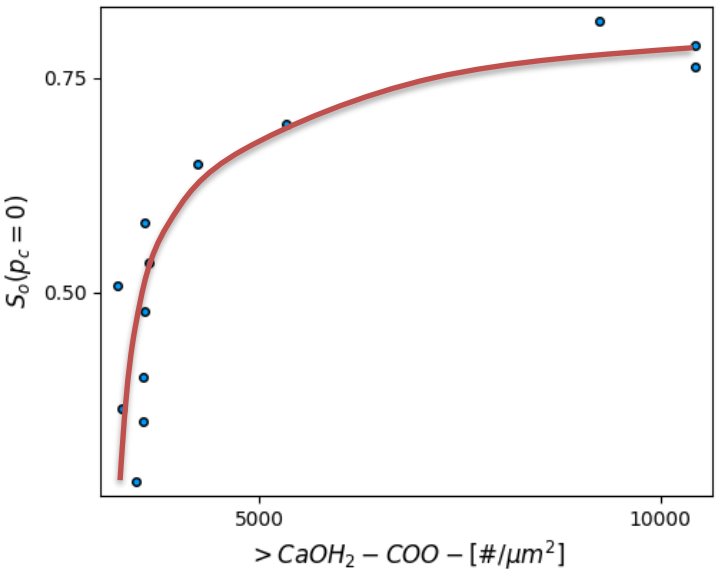

Figure 7. The relation between the oil recovery (shown as the oil saturation at p_c=0) with the number of bonds between the carboxylate ion on the oil phase and the protonated calcium site on the chalk surface; the solid lines only shows the trend of the data and is not an actual fit. The experimental data is obtained from Fathi et al. [1].

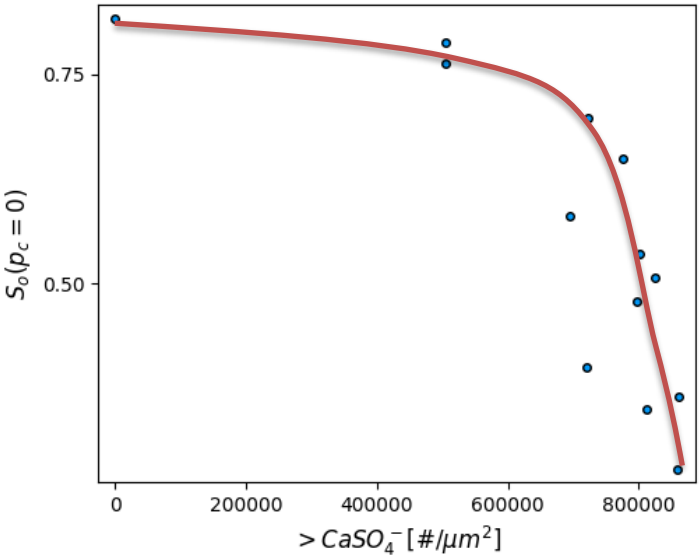

Figure 8. The measured remaining oil saturation in the imbibition tests of Fathi et al. [1] versus the calculated concentration of adsorbed sulfate on the chalk surface.

Figure 9-a and -b show the measured remaining oil saturation in the imbibition experiments of Zhang et al.[34] versus the calculated calcium-carboxylate and carbonate-amine bonds between the surface of chalk and oil, respectively. The total number of acid-base bonds, which is the summation of the calcium-carboxylate and carbonate-amine bonds are shown in Figure 9. Once again, a correlation can be observed between the number of bonds and the amount of oil that is left behind in the imbibition experiments, even with the different types of oil that are used by Zhang et al. [34]. There are a number of data points that do not follow, marked by a dashed square in Figure 8-a and -b that do not follow the observed trend, that requires further investigation.

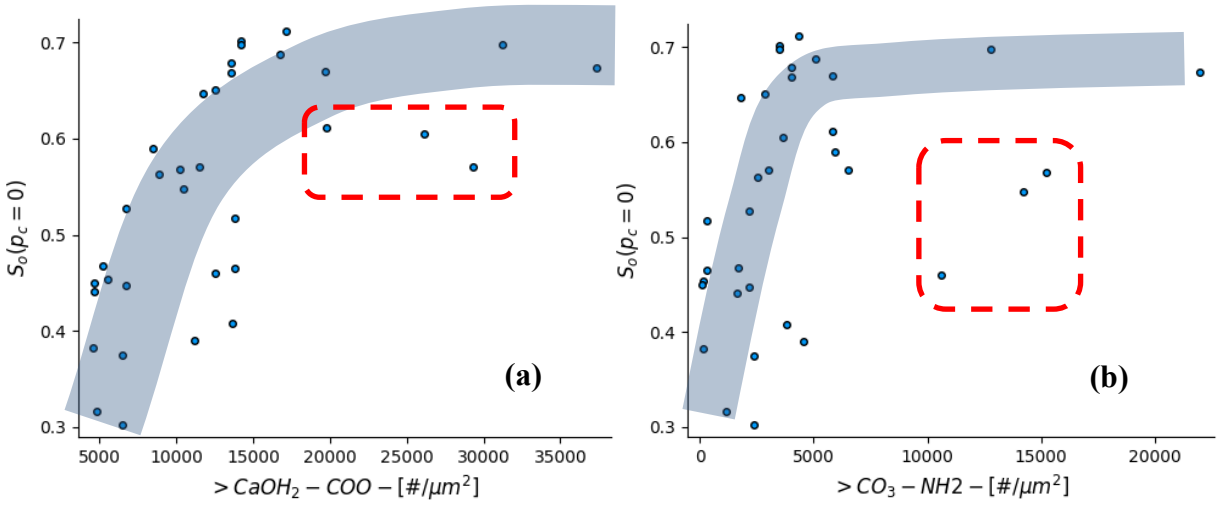

Figure 9. The calcium-carboxylate and carbonate-amine bonds between the chalk and the oil surfaces versus the remaining oil saturation in the imbibition experiments of Zhang et al.[34]. The oil contains both acidic and basic components.

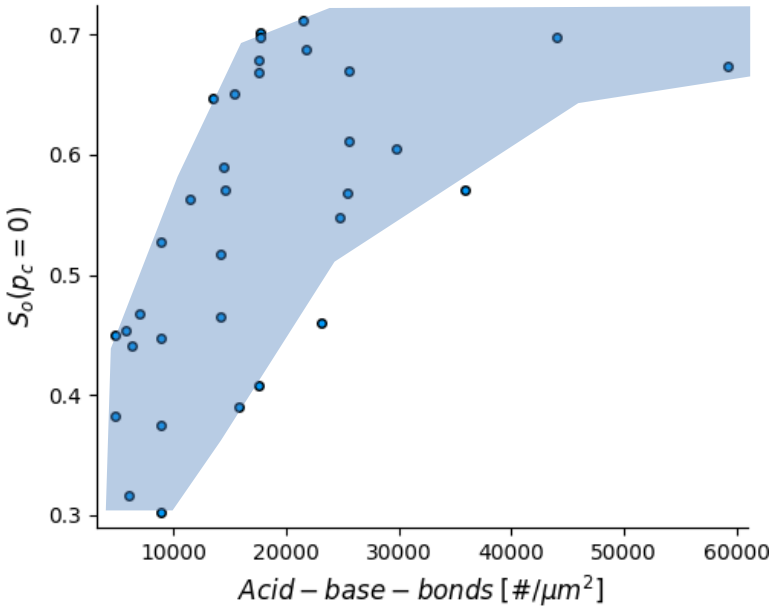

Figure 10. Measured remaining oil saturation in the imbibition experiments[34] versus the calculated total number of acid-base bonds between the chalk and the oil surfaces.

We must point out that the correlation shown in Figure 7 and Figure 10 does not necessarily indicate that we have discovered the true mechanism behind the effectiveness of the modified

salinity water flooding. However, it is one step further towards the derivation of a mechanistic model with fewer empirical relations and parameters.

Conclusions

In this work, we present a diffuse-layer surface complexation model to describe the chemical interactions in the chalk-brine-oil system, including the adsorption of oil and chalk and the dissolution/precipitation of carbonate and anhydrite. The key findings of this study are as follows:

- At lower pressure and at the reservoir temperature, the simple Davies model is adequate for the prediction of the solubility of anhydrite and calcite. At higher pressures, more sophisticated and computationally expensive alternatives need to be considered.
- The equilibrium constants for the surface complexation reactions that are reported in the literature are measured for the pure crystalline calcite and are not able to predict the zeta potential of chalk particles in brine.
- The reaction equilibrium constants that are fitted to the measured zeta potential of pulverized chalk in brine are not suitable for modeling the reactive transport of brine in chalk. The parameters need to be tuned to fit the breakthrough curves of different ions.
- The presence of small amounts of clay particles reduces the calculated surface charge and zeta potential of the chalk surface, but does not considerably affect the adsorption of the potential determining ions (Ca and Mg) on the chalk surface.
- A correlation between the remaining oil in the imbibition tests and the number of bonds between the carboxylate group on the oil surface and the protonated calcium sites on the chalk surface is suggested based on the developed model and the tuned parameters.

ACKNOWLEDGMENT

The research leading to these results has received funding from the Danish Hydrocarbon Research and Technology Centre under the Advanced Water Flooding programme. AAE would like to thank David Parkhurst for his helpful comments on the utilization of the SCM models in PHREEQC. The very valuable comments of the anonymous reviewer are greatly appreciated.

ABBREVIATIONS

SCM, Surface Complexation Model.

PV. Pore Volumes

REFERENCES

(1) Fathi, S. J.; Austad, T.; Strand, S. *Energy Fuels* **2010**, *24* (4), 2514–2519.
(2) Sohal, M. A.; Thyne, G.; Søgaard, E. G. *Energy Fuels* **2016**, *30* (3), 1904–1914.
(3) Zahid, A.; Shapiro, A. A.; Skauge, A.; others. In *SPE EOR Conference at Oil and Gas West Asia*; Society of Petroleum Engineers, 2012.
(4) Zhang, P.; Austad, T. *Colloids Surf. Physicochem. Eng. Asp.* **2006**, *279* (1), 179–187.
(5) Chakravarty, K. H.; Fosbøl, P. L.; Thomsen, K.; others. In *SPE Bergen One Day Seminar*; Society of Petroleum Engineers, 2015.
(6) Morrow, N.; Buckley, J.; others. *J. Pet. Technol.* **2011**, *63* (05), 106–112.
(7) Hiorth, A.; Cathles, L.; Madland, M. *Transp. Porous Media* **2010**, *85* (1), 1–21.
(8) Brady, P. V.; Krumhansl, J. L.; Mariner, P. E.; others. In *SPE Improved Oil Recovery Symposium*; Society of Petroleum Engineers, 2012.
(9) Brady, P. V.; Thyne, G. *Energy Fuels* **2016**, *30* (11), 9217–9225.
(10) Lager, A.; Webb, K.; Black, C.; Singleton, M.; Sorbie, K.; others. *Petrophysics* **2008**, *49* (01).
(11) Dang, C.; Nghiem, L.; Nguyen, N.; Chen, Z.; Nguyen, Q. *J. Pet. Sci. Eng.* **2016**, *146*, 191–209.
(12) Kazemi Nia Korrani, A.; Jerauld, G. R.; Sepehrnoori, K.; others. *SPE Reserv. Eval. Eng.* **2016**.
(13) Qiao, C.; Johns, R. T.; Li, L. *Energy Fuels* **2016**.
(14) Qiao, C.; Li, L.; Johns, R. T.; Xu, J.; others. *SPE J.* **2015**.
(15) Van Cappellen, P.; Charlet, L.; Stumm, W.; Wersin, P. *Geochim. Cosmochim. Acta* **1993**, *57* (15), 3505–3518.
(16) Wolthers, M.; Charlet, L.; Van Cappellen, P. *Am. J. Sci.* **2008**, *308* (8), 905–941.
(17) Goldberg, S. *Surface complexation modeling. in Reference Module in Earth Systems and Environmental Sciences*; Elsevier, 2013; Vol. 10.
(18) Hjuler, M. L.; Fabricius, I. L. *J. Pet. Sci. Eng.* **2009**, *68* (3), 151–170.
(19) Strand, S.; Hjuler, M. L.; Torsvik, R.; Pedersen, J. I.; Madland, M. V.; Austad, T. *Pet. Geosci.* **2007**, *13* (1), 69–80.

(20) Lindgreen, H.; Drits, V. A.; Sakharov, B. A.; Jakobsen, H. J.; Salyn, A. L.; Dainyak, L. G.; Krøyer, H. *Clay Miner.* **2002**, *37* (3), 429–450.
(21) Buckley, J. S. In *Proc. 3 rd International Symposium on Evaluation of Reservoir Wettability and Its Effect on Oil Recovery*; 1994; pp 33–38.
(22) Pokrovsky, O. S.; Schott, J.; Thomas, F. *Geochim. Cosmochim. Acta* **1999**, *63* (19–20), 3133–3143.
(23) Brady, P. V.; Krumhansl, J. L. *J. Pet. Sci. Eng.* **2012**, *81*, 171–176.
(24) Pokrovsky, O.; Schott, J. *Environ. Sci. Technol.* **2002**, *36* (3), 426–432.
(25) Megawati, M.; Hiorth, A.; Madland, M. V. *Rock Mech. Rock Eng.* **2013**, *46* (5), 1073–1090.
(26) Zeinijahromi, A.; Nguyen, T. K. P.; Bedrikovetsky, P.; others. *SPE J.* **2013**, *18* (03), 518–533.
(27) Davies, C. W. *J. Chem. Soc. Resumed* **1938**, 2093–2098.
(28) Pitzer, K. S. *J. Phys. Chem.* **1973**, *77* (2), 268–277.
(29) Sander, B.; Rasmussen, P.; Fredenslund, A. *Chem. Eng. Sci.* **1986**, *41* (5), 1197–1202.
(30) García, A. V.; Thomsen, K.; Stenby, E. H. *Geothermics* **2005**, *34* (1), 61–97.
(31) García, A. V.; Thomsen, K.; Stenby, E. H. *Geothermics* **2006**, *35* (3), 239–284.
(32) Buckley, J.; Liu, Y.; Monsterleet, S.; others. *SPE J.* **1998**, *3* (01), 54–61.
(33) Parkhurst, D. L.; Appelo, C.; others. **1999**.
(34) Zhang, P.; Tweheyo, M. T.; Austad, T. *Colloids Surf. Physicochem. Eng. Asp.* **2007**, *301* (1), 199–208.
(35) Zhang, P.; Tweheyo, M. T.; Austad, T. *Energy Fuels* **2006**, *20* (5), 2056–2062.
(36) Yutkin, M. P.; Lee, J. Y.; Mishra, H.; Radke, C. J.; Patzek, T. W.; others. In *SPE Kingdom of Saudi Arabia Annual Technical Symposium and Exhibition*; Society of Petroleum Engineers, 2016.
(37) Jackson, M. D.; Al-Mahrouqi, D.; Vinogradov, J. *Sci. Rep.* **2016**, *6*.
(38) Mahani, H.; Keya, A. L.; Berg, S.; Nasralla, R.; others. *SPE J.* **2016**.
(39) Mahani, H.; Keya, A. L.; Berg, S.; Bartels, W.-B.; Nasralla, R.; Rossen, W. R. *Energy Fuels* **2015**, *29* (3), 1352–1367.
(40) Bezanson, J.; Edelman, A.; Karpinski, S.; Shah, V. B. *ArXiv Prepr. ArXiv14111607* **2014**.
(41) Parkhurst, D. L.; Wissmeier, L. *Adv. Water Resour.* **2015**, *83*, 176–189.
(42) Eftekhari, A. A. JPhreeqc.jl https://github.com/simulkade/JPhreeqc.jl (accessed Dec 9, 2016).
(43) Kraft, D. *ACM Trans. Math. Softw. TOMS* **1994**, *20* (3), 262–281.
(44) Kraft, D.; others. *A software package for sequential quadratic programming*; DFVLR Obersfaffeuhofen, Germany, 1988.
(45) Johnson, S. G. *The NLopt nonlinear-optimization package*; 2015.
(46) Brady, P. V.; Krumhansl, J. L.; others. *SPE J.* **2013**, *18* (02), 214–218.
(47) Strand, S.; Standnes, D.; Austad, T. *J. Pet. Sci. Eng.* **2006**, *52* (1), 187–197.
(48) Eftekhari, A. A.; Krastev, R.; Farajzadeh, R. *Ind. Eng. Chem. Res.* **2015**.
(49) Song, J.; Zeng, Y.; Wang, L.; Duan, X.; Puerto, M.; Chapman, W. G.; Biswal, S. L.; Hirasaki, G. J. *J. Colloid Interface Sci.* **2017**, *506*, 169–179.
(50) Appelo, C. *Appl. Geochem.* **2015**, *55*, 62–71.
(51) Robinson, R. A.; Stokes, R. H. *Electrolyte solutions*; Courier Corporation, 2002.
(52) Thomsen, K.; Rasmussen, P. *Chem. Eng. Sci.* **1999**, *54* (12), 1787–1802.

(53) Nick, H.; Raoof, A.; Centler, F.; Thullner, M.; Regnier, P. *J. Contam. Hydrol.* **2013**, *145*, 90–104.
(54) Puntervold, T.; Strand, S.; Austad, T. *Energy Fuels* **2007**, *21* (6), 3425–3430.